

# A NEW MODEL OF THE INTERNATIONAL REFERENCE IONOSPHERE IRI FOR TELECOMMUNICATION AND NAVIGATION SYSTEMS

Olga Maltseva, Natalia Mozhaeva, Gennadyi Zhbakov

*Institute of Physics Southern Federal University, Stachki, 194, Rostov-on-Don, Russia*

*mal@ip.rsu.ru, mozh\_75@mail.ru, zhbakov\_ga@rambler.ru*

**Keywords:** GPS. Total electron content. Ionospheric model. Radio wave propagation. Geomagnetic disturbances.

**Abstract:** Telecommunication, navigation, positioning systems require knowledge of ionospheric Ne(h)-profiles up to high-altitude orbits of satellites. The only way to construct such profiles is associated with the use of the ionospheric total electron content TEC. New option IRI-Plas of the IRI2010 model allows us to construct Ne(h)-profiles by adjustment of the model to the current maximum values of the parameters of the ionospheric F2 layer ( $f_0F2$ ,  $hmF2$ ) and the TEC. This paper contains a comprehensive comparison of these profiles with the data of various experiments (ISR, CHAMP, DMSP). Results show the high efficiency of this adjustment. The proposed method of further adjustment of the IRI-Plas model to the plasma frequency at altitudes of CHAMP and DMSP satellites allows us to produce behaviors of Ne(h)-profiles during the disturbances, as well as to refine the values of TEC, which determine the accuracy of positioning.

## 1 INTRODUCTION

The operation of the various satellite communication, navigation, global positioning systems (GPS) depends on the state of the ionosphere and needs to know the electron distribution in height (Ne(h)-profiles) in near space. Methods for direct measurement of the Ne(h) at these altitudes are not exist, however, there are a number of theoretical and empirical models of Ne(h)-profiles. In many applications of radio and satellite communications, the empirical model of the ionosphere IRI (Bilitza, 2001; 2006) is most widely used, but it determines the Ne(h)-profile to a height of 2000 km. Ability to determine the profiles at high altitudes is associated with the total electron content (TEC) of the ionosphere. This parameter is defined as the number of electrons in the atmospheric column, measured by the navigation satellites (GPS, etc.) and directly related to the Ne(h)-profiles of the ionosphere. Despite the difficulties in determining the TEC (slips of signal phase, an idealization of the model of the ionosphere on the conversion of slant TEC into the vertical VTEC, the dependence on the type of receiver, etc.), it is widely used in various applications. However, the IRI model gives a large discrepancy when compared with the experimental TEC because of the profile shape of the topside

ionosphere (e.g., Stankov et al., 2003; Uemoto et al. 2007; Bilitza, 2009; Maltseva et al., 2011), so that the model has been modified several times in this century (IRI2001 (Bilitza, 2001), IRI2007 (Bilitza and Reinish, 2006; 2008)) and modification continues. In 2010, a new version IRI2010 (Bilitza et al., 2010) of the IRI model was proposed, which included a model of T. Gulyaeva. Although this model has been developed for a long time, for example (Gulyaeva et al., 2002; Gulyaeva, 2003), it is formally incorporated as IRI-Plas just now. The main advantages of this model are accounting a plasmaspheric part of the magnetosphere, and the ability to be adapted to the experimental parameters of the ionosphere (the critical frequency  $f_0F2$ , the maximum height  $hmF2$ , TEC). This should allow us to determine the shape of Ne(h)-profiles. The purpose of this paper are: 1) validation of the IRI-Plas model according to various experiments (incoherent sounding radars ISR, satellite CHAMP ( $hsat \sim 400$  km) and DMSP measurements ( $hsat \sim 800$  km)), 2) validation of the IRI-Plas model according to the particular ionospheric station of Sofia, 3) determination of the behavior of Ne(h) profiles during the disturbed conditions, 4) refinement of the values of TEC by means of further adaptation of the model to the plasma frequency at altitudes of satellites CHAMP and DMSP. These results may

have important implications for telecommunication, navigation, positioning systems.

## 2 ON THE IRI MODEL

As noted in (Bilitza, 2006), “The International Reference Ionosphere (IRI) project was initiated by the Committee on Space Research (COSPAR) and by the International Union of Radio Science (URSI) in the late sixties with the goal of establishing an international standard for the specification of ionospheric parameters based on all worldwide available data from ground-based as well as satellite observations. COSPAR and URSI specifically asked for an empirical data-based model to avoid the uncertainties of the evolving theoretical understanding of ionospheric processes. COSPAR’s main interest is in a general description of the ionosphere as part of the terrestrial environment for the evaluation of environmental effects on spacecraft and experiments in space. URSI’s prime interest is in the electron density part of IRI for defining the background ionosphere for radiowave propagation studies and applications. To accomplish these goals a joint COSPAR-URSI Working Group was established and tasked with the development of the model.” IRI describes monthly averages of the electron density, electron temperature, ion composition ( $O^+$ ,  $H^+$ ,  $N^+$ ,  $He^+$ ,  $O_2^+$ ,  $NO^+$ , Cluster+), ion temperature, and ion drift in the ionospheric altitude range (60 km to 1000 km). Some of the primary applications are listed in Table 1 in (Bilitza, 2006) together with typical usage examples. The model is recommended as the ionospheric standard. The model is located on the site: <http://modelweb.gsfc.nasa.gov/ionos/iri.html>. The maximum parameters (foF2, hmF2) are provided by the ITU-R (former CCIR) or URSI maps. Drivers of the model are parameters characterizing solar and geomagnetic activity (RZ12, IG12, ap and others). Input parameters are day, month, year, coordinates of the point among others. TEC is calculated by the formula  $TEC = \int N_e dh$ . The calculation ceiling of previous versions was 2000 km. The IRI-Plas model extended to the plasmasphere. Output parameters important for our purposes are the critical frequency foF2, the maximum height hmF2, TEC, Ne(h)-profiles. All versions provide adaptation of the model to current values of foF2, hmF2 and include the STORM-factor adapting the model to disturbed conditions (Araujo-Pradere et al. 2004).

## 3 VALIDATION OF THE IRI-PLAS MODEL ACCORDING TO DIFFERENT EXPERIMENTS

Experimental values of the parameters foF2 and hmF2 are taken from the SPIDR database. TEC values are computed from IONEX files of the global maps delivered online by four organizations: JPL (Mannucci et al., 1998), CODE (Schaer et al., 1995), UPC (Hernandez-Pajares et al., 1999), ESA (Sardon et al., 1994; Jakowski et al., 1996). Ne(h)-profiles of incoherent sounding radars for six stations are taken from (Zhang et al., 2007). These profiles show the Ne to a height of 500 km. In all cases, the coincidence of the model and experimental profiles was good. Quantitative results are presented in Table 1 in the form of the experimental and calculated values of the plasma frequency fne at an altitude of 500 km for the three European radars. These radars are Svalbard (78.1°N, 16°E), StSantin (44.6°N, 2.2°E), Tromso (69.6°N, 19.2°E). The first column gives the shortening name of the station and the day of measurement (1 = 03/31/1999, 2 = 29/07/1999, 3 = 11/26/2002). Data of (Zhang et al., 2007) refer to LT = 12, but calculations were done for UT corresponding to each radar. The following columns represent the results of different calculations, which should be compared with values in the last column (ISR) containing experimental ones. The results show that the model and experimental profiles match very well, but we can not specify a map, which would be consistent with all experiments, so it is advisable to choose a map that gives the closest value of fne.

Table 1: Comparison of the IRI-Plas model results with ISR data of three radars

	IRI	foF2	TEC	JPL	ESA	ISR
Sv(1)	3.57	2.37	3.37	3.35	3.33	3.19
Sv(2)	2.86	2.64	3.77	3.75	2.53	3.79
Sv(3)	2.84	1.57	1.62	2.22	2.15	2.01
St(1)	5.52	3.46	3.10	4.19	2.43	4.01
St(2)	3.57	2.70	3.09	3.85	3.42	4.01
St(3)	4.49	3.16	2.33	3.66	3.04	3.38
Tr(1)	4.00	2.37	2.24	2.74	0.71	3.66
Tr(2)	2.86	3.05	3.79	3.94	3.52	3.79
Tr(3)	3.50	2.47	1.59	2.41	2.37	3.38

## 4 VALIDATION OF THE IRI-PLAS MODEL ACCORDING TO DATA OF THE SOFIA STATION

Data of the Sofia station were selected to demonstrate results of validation of the IRI-Plas model and to show its new possibilities. Validation is carried out for four cases: (1) the original model IRI, (2) the IRI model, adapted to the experimental value of foF2, (3) the IRI model, adapted to the experimental value of the TEC, (4) the IRI model, adapted to the experimental values of foF2 and TEC, to show the difference between the results for these methods. Option 1 is used when there is no current information and determines the average ionospheric state. It is a standard for comparison with other options. Option 2 uses the current value of foF2 and completely defines the bottom part of the profile. Option 3 is widely used in connection with the TEC measurements with navigation satellites. The advantage of this option before the second one is in a continuous global monitoring. Adapting the model to the current values of the TEC allows us to obtain new (reconstructed) values of foF2. Option 4, as stated in the introduction, is one of the main differences between the new IRI model and previous versions. It allows to determine the Ne(h)-profile at the location of ionosondes. Validation of these options is to compare the plasma frequency at altitudes of satellites calculated for the model with the experimental values of fne. A comparison was carried out for two satellites CHAMP (hsat  $\sim$  400 km) and DMSP (hsat  $\sim$  840 km). Data of foF2 are taken from SPIDR, values of TEC – from global maps of JPL, CODE, UPC, ESA. Results are presented for April 2001 including two strong disturbances (1-2 April with minimum Dst=-228 nT and 11-12 April with minimum Dst=-273 nT) and two weak disturbances (18 and 22-23 April) with minimum Dst $\sim$ 100 nT. Table 2 shows the results of comparisons of Ne(h)-profiles with satellite CHAMP data. Table includes day, time of observation, and the values of plasma frequencies for the respective versions and the CHAMP satellite. Figures in round brackets indicate numbers of options. The last column shows fne of the CHAMP satellite. Heights of the satellite were in range 410-460 km.

The best fit of model and the experimental values is provided by the fourth version. Examples of the profiles are shown in Fig. 1a, b. Fig. 1a presents night profiles (UT=1), Fig. 1b presents daytime profiles (UT=13). Examples for night

profiles are given for cases of  $\text{foF2}(\text{obs}) > \text{foF2}(\text{IRI})$  (the left panel) and  $\text{foF2}(\text{obs}) < \text{foF2}(\text{IRI})$  (the right panel).

Figures in round brackets after the name of the satellite indicate a time of observation if this time does not coincide with data of TEC. Values of the model and satellite plasma frequencies coincide for the forth version.

Table 2: Comparison of simulation results for different versions of the IRI model with the data of the CHAMP satellite

day	UT	IRI (1)	foF2 (2)	TEC (3)	All (4)	CH fne
3	1	5.57	6.45	5.75	6.44	6.50
3	13.1	9.27	10.70	10.14	10.94	11.14
6	12.6	9.33	9.97	9.84	10.15	10.01
11	0.4	5.72	5.07	5.41	5.06	5.04
13	12.6	9.16	11.09	9.96	10.87	11.16
19	23	6.51	5.02	5.07	4.92	4.37
21	23.2	6.52	6.53	6.45	6.46	6.21
23	23.4	6.52	5.80	5.91	5.67	5.35
24	22.7	6.53	6.15	6.30	6.11	6.00
26	22.9	6.53	6.53	6.55	6.55	6.92
29	11.2	8.14	8.88	8.60	8.65	8.74
29	22.5	6.54	5.85	6.04	5.78	5.74
30	10.5	8.10	8.05	8.21	8.20	7.76

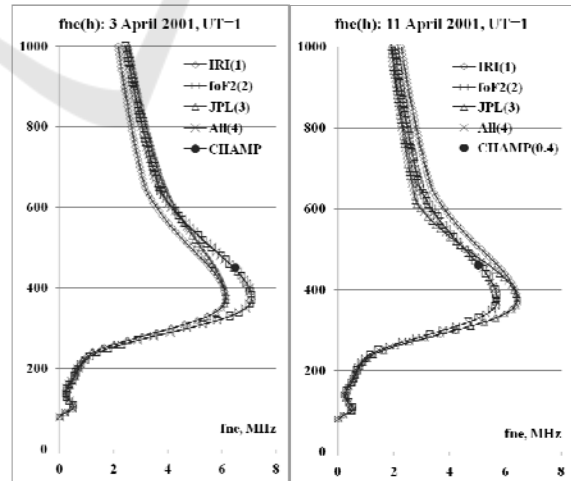


Figure 1a: Comparison of model Ne(h)-profiles and the results for the CHAMP satellite (April 2001) for night time

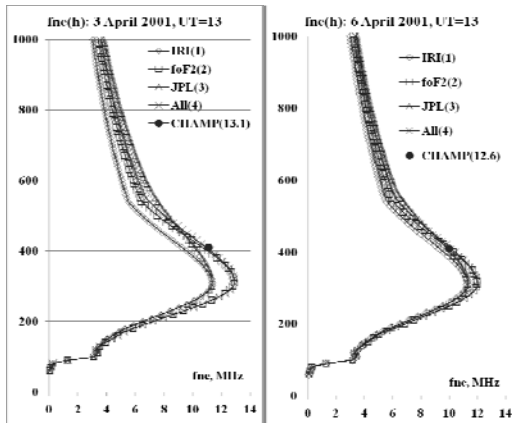


Figure 1b: Comparison of model  $Ne(h)$ -profiles and the results for the CHAMP satellite (April 2001) for day time

The same correspondence can be seen for the noon time profiles, although the time of the satellite flight is slightly different from the time of measurement of ionospheric parameters. Exact coincidence of these times is rare.

More often are the cases when the satellite passed over the station at even hours, whereas the values of TEC were only for the odd hours. Typical examples of calculations for these cases are shown in Fig. 2 for daytime and nighttime profiles for the forth option (full adjustment).

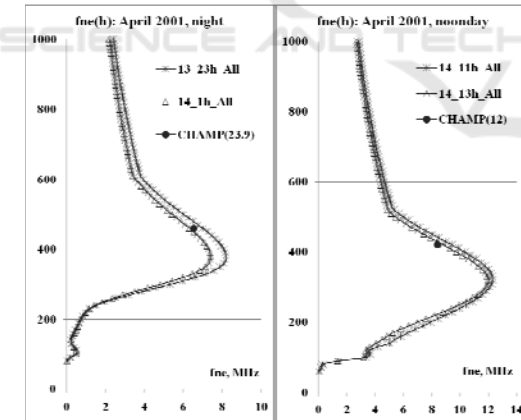


Figure 2: The cases of the satellite flight in the average hours between the measurements of the TEC

Orbit heights of DMSP satellites exceed 800 km. The results using data of DMSP were obtained under the same scenario. In this case data of three satellites were available (F12, F13, F15). Typical results are shown in the Table 3. They present plasma frequencies for four options and experimental values  $fne$ .

Table 3: Comparison of simulation results for different versions of the IRI model with data of DMSP satellites ( $h_{sat} \sim 840-860$  km)

day	UT	IRI (1)	foF2 (2)	JPL (3)	All (4)	fne
1	5.5	2.10	1.22	1.71	2.07	2.15
1	8.7	3.46	2.73	2.88	3.40	2.71
1	15.3	3.32	3.17	3.67	3.76	3.36
1	17.4	3.10	2.95	3.61	3.67	3.02
2	5.3	2.13	2.13	2.77	2.77	2.38
2	7.5	2.76	3.00	3.74	3.62	2.94
2	17.2	3.11	3.41	3.77	3.61	2.75
3	7.3	2.77	3.28	4.06	3.79	2.89
3	8.2	3.47	4.03	4.68	4.35	3.41
3	16.5	3.15	3.69	4.20	3.92	3.33
4	4.9	2.15	2.73	3.44	3.22	2.76
4	7	2.77	3.17	3.97	3.77	3.04
4	19.4	2.96	3.38	3.89	3.70	3.44
5	19.2	2.97	2.87	3.31	3.35	2.81
11	19.4	3.04	3.60	3.60	3.27	3.52
12	4.8	2.23	1.39	1.38	1.95	1.73
12	7	2.82	1.69	1.93	2.64	2.19
12	19.2	3.05	2.75	2.45	2.68	1.60
13	4.6	2.24	2.08	2.19	2.29	1.80

The distinction of this case is the fact that the best agreement between the calculated and experimental values of  $fne$  is obtained for the original model or adaption of the model to current  $foF2$ . Using the experimental values of TEC leads to overvalued values of  $fne$ . A too high value for the map of JPL should be considered as a possible cause. This can be confirmed by the results for other maps presented in Fig. 3. Experimental plasma frequencies  $fne$  are shown by full points, the other values are corresponding to various maps.

It is seen that often experimental frequencies do not reach range of map values. Nevertheless, the agreement between the calculated and experimental values of  $fne$  exists. Typical examples of  $Ne(h)$ -profiles are shown in Fig. 4 as close to the moment of the flight time and for the middle of two hour period.

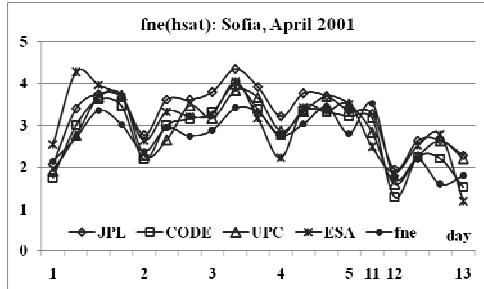


Figure 3: Comparison of experimental plasma frequencies  $f_{\text{ne}}$  and frequencies provided by maps of JPL, CODE, UPC, ESA

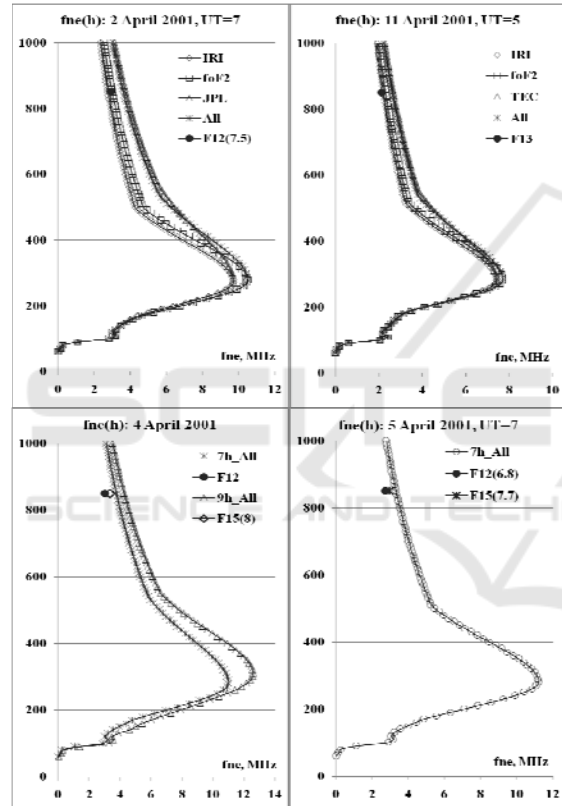


Figure 4: Comparison of model  $Ne(h)$ -profiles and the results of the DMSP satellite (April 2001)

## 5 EXAMPLES OF THE BEHAVIOR OF $Ne(h)$ -PROFILES AT THE SOFIA STATION DURING DISTURBANCES

The results of the previous section show that the profiles are rather well adapted to meet the satellite measurements. This allows us to study and simulate

the height distribution of the ionospheric ionization. The choice of  $Ne(h)$ -profiles in the previous section was dictated by time of flight of the satellite. For a variety of tasks long periods of observation are important especially for disturbed conditions when the profiles can be strongly modified. Examples of the behavior of  $Ne(h)$ -profiles for the longitudinal (left panels) and latitudinal (right panels) chains connected with the Sofia station are shown in Fig. 5. The upper two sets of graphs display night profiles ( $UT = 1$ ), the bottom two groups – daytime profiles ( $UT=11$ ). The upper graphs of each group show the profiles during quiet conditions, the lower profiles - in the disturbed ones. In the night of 12 April, quiet conditions on the longitudinal chain (Sodankyla, Leningrad, Moscow, Sofia) are presented by  $Ne(h)$ -profiles of the IRI model. We can see the coincidence of the values of three northern stations and high values for Sofia because it is the most southerly. During the disturbance, which is negative, the profiles vary strongly, because all the ionospheric structures are shifted to the south. Thus, the Moscow station is in the area of the ionospheric trough, the Leningrad station falls from the plasmaspheric area into zone of subauroral amplification. The most strongly reduced is the concentration at the Sofia station reaching values less even than the values in the subauroral Sodankylä station. This leads to huge gradients of the electron concentration that must be considered in the propagation of radio waves. On the latitudinal chain (Sofia, Rome, Ebre), profiles of the Sofia station have the lowest ionization, indicating a positive gradient towards lower latitudes under quiet conditions. During the negative disturbance, a decrease in the concentration at all the stations can reduce gradients. During the day, the concentration distribution in the quiet time should be clearly decreased with increasing latitude. An example of the lower grafts shows that a positive (in this case) perturbation has the greatest effect on the concentration of the Sofia station. Example of daytime profiles for a quiet state and during the April 3 disturbance is shown in the lower right-hand chart. It is seen that if a negative disturbance during the night enveloped almost the entire European region, the daytime disturbance may influence by different manner at various stations.

Since the bottom and topside parts of the profile may respond differently to disturbance, such profiles can provide a quantitative assessment of effects of disturbances.

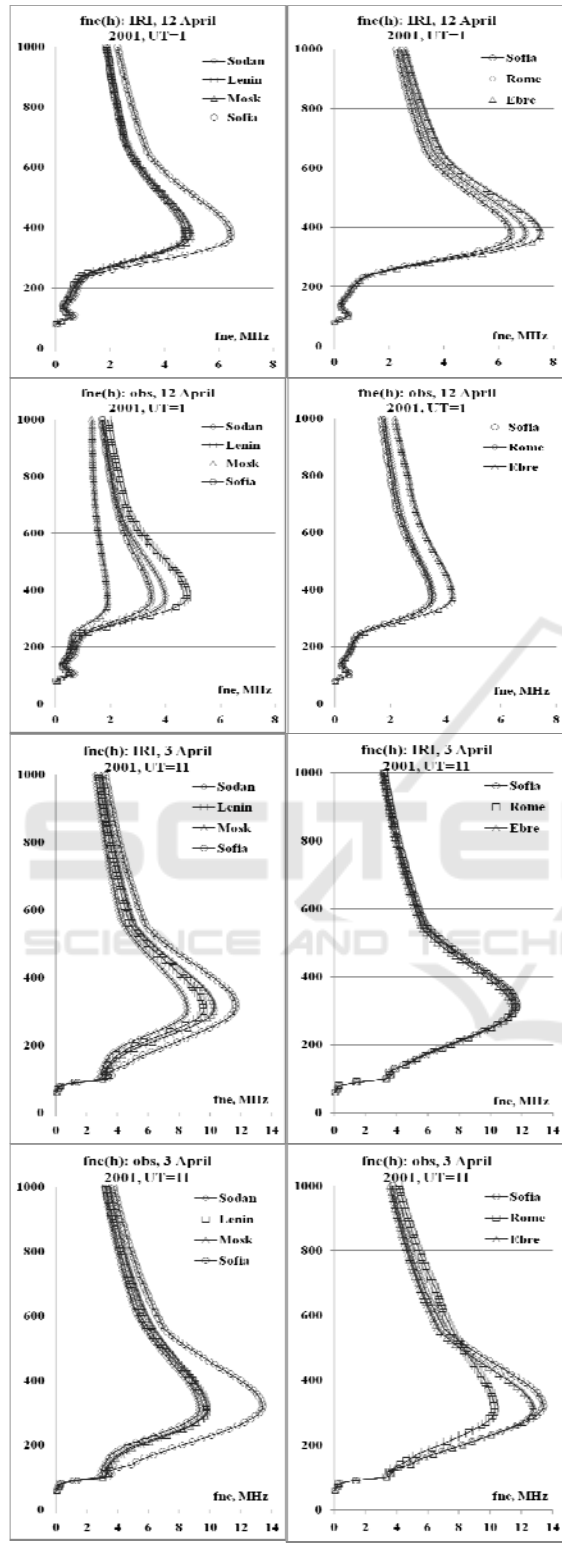


Figure 5: Sequence of  $N_e(h)$ -profiles showing their modification during the disturbances

## 6 CASES OF LACK OF MEASUREMENT OF IONOSPHERIC PARAMETERS AT THE STATION

In the absence of measurements of ionospheric parameters at the station there are at least two methods to obtain  $N_e(h)$ -profiles: (1) the use of the parameters of the original model, (2) the use of the median equivalent thickness of the ionosphere  $\tau(\text{med})$  in conjunction with the TEC. The first option coincides with the first option of the section 4 and provides good results for the conditions close to the quiet ones, but during the disturbances difference can be substantial, as illustrated in Fig. 6. Fig. 6 shows the results of calculations for all versions. It is evident that the difference is significant, not only near the peak of the layer F2, but at the top of the profile. The full points indicate the plasma frequency of DMSP satellites.

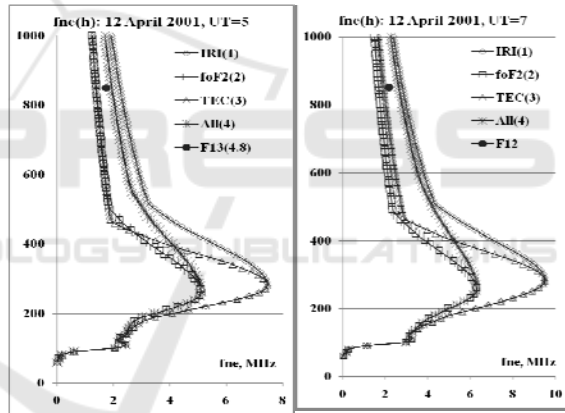


Figure 6: Comparison of  $N_e(h)$ -profiles in the case of strong differences in  $f_{oF2}$  (IRI) and  $f_{oF2}$  (obs), caused by a disturbance

These two successive profiles show an increase in the diurnal  $f_{oF2}$ , but the perturbation has a strong influence. Therefore, it is preferable to use the second method. In (Maltseva et al., 2012) is shown that the use of the median equivalent thickness of the ionosphere  $\tau(\text{med})$  in conjunction with the TEC allows us to fill in gaps in the data by means of using reconstructed values of  $f_{oF2}$ . The effectiveness of this approach is estimated using the deviations of the calculated and experimental values of  $f_{oF2}$  for periods when there are complete data sets. For four disturbed periods in April 2001 for the Sofia station, these deviations are shown in Fig. 7.

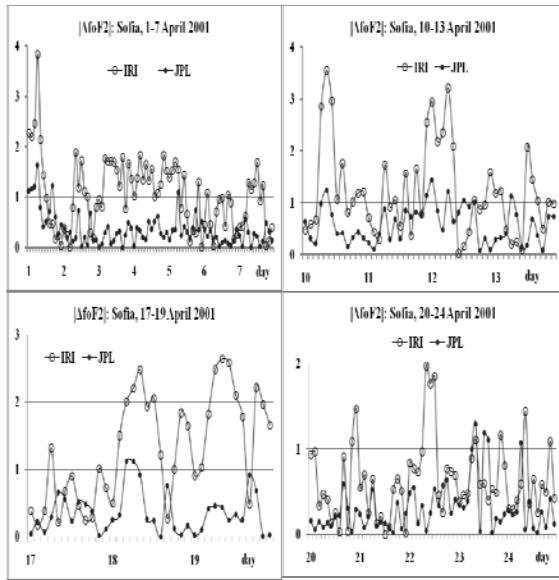


Figure 7: Deviations of the model and reconstructed values of foF2 from the experimental ones

It is seen that the greatest deviations of model foF2 values from the experimental ones account for the days of disturbances. Using  $\tau(\text{med})$  in conjunction with the TEC can increase compliance by many times. This section contains attempts to do the next step: to use  $\tau(\text{med})$  of one (reference) stations for the determination of foF2 of another station from its values of TEC. We validate this procedure with the help of satellite data. The results are shown in the example of May 2005, which was also marked by four disturbances with minimal index Dst:-127nT (8.05), -263nT (15.05), -103nT (20.5), -138nT (30.5). For the Sofia station, ionospheric observation data are absent in the SPIDR database since 2005. Rostov was chosen as the reference station to determine the values of foF2 for the Sofia station. Values of  $\tau(\text{med})$  of the Rostov station and TEC values of the Sofia station are used. To be sure in correctness of using  $\tau(\text{med})$  of the Rostov station we compared  $\tau(\text{med})$  of these stations for some previous years. Fig. 8 displays experimental and model values of median equivalent thickness  $\tau$  of the ionosphere for stations of Sofia and Rostov in May of those years for which measurements were available simultaneously at both stations in the SPIDR. Model values (sign IRI) shown by the triangles and asterisks coincide. Namely these values are used in traditional methods of determining foF2 from TEC (McNamara, 1985; Houminer and Soicher, 1996, Gulyaeva, 2003). They ensure deviations between experimental and model values of foF2 shown in Fig. 7 by circles. The more important fact is the

closeness of the experimental values of  $\tau(\text{med})$  for both stations. Using these values ensures deviations shown in Fig. 7 by points.

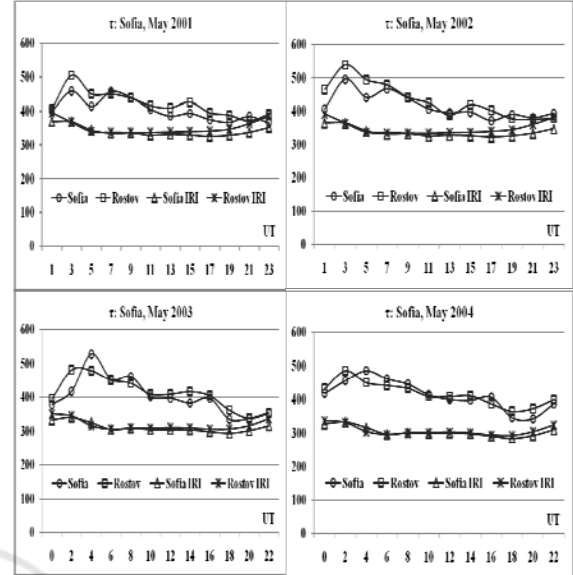


Figure 8: Comparison of equivalent thicknesses  $\tau$  for Sofia station

Table 4: Comparison of simulation results for different versions of the IRI model with the data of CHAMP satellite in May 2005 (hsat~860 km)

day	UT	IRI	foF2	TEC	All	fne
1	9	5.73	5.69	5.95	5.93	5.41
2	21.3	4.82	3.67	4.76	3.70	3.91
3	8.4	4.99	5.33	5.48	5.65	5.45
4	20.7	5.69	5.31	5.66	5.34	3.99
6	8.3	4.97	5.33	5.47	5.65	4.59
12	8	4.91	5.34	5.44	5.66	4.55
12	19.9	5.87	5.97	5.99	6.07	6.02
18	19.6	5.96	5.08	5.77	5.15	4.87
21	19.5	5.97	5.38	5.93	5.48	5.27
23	7.1	4.88	4.97	5.26	5.30	3.81
24	19.3	5.99	5.83	6.09	5.95	5.78
28	6.3	4.65	5.59	5.34	5.93	5.46
28	18.5	6.07	6.45	6.41	6.72	6.55
29	18.6	6.06	6.38	6.39	6.65	7.05
30	5.7	4.65	4.48	4.89	4.81	4.07

The profiles obtained using the reconstructed values of foF2 are compared with data of CHAMP and

DMSP satellites. The results are shown in Tables 4-5 separately for each satellite. In this case, there were more flights with similar times for both satellites, so in the Table 5 we focus on the close passages.

Table 5: Comparison of simulation results for different versions of the IRI model with data of DMSP satellites in May 2005 (hsat~840 km).

day	UT	IRI	foF2	TEC	All	fne
1	7.2	1.89	1.99	2.33	2.29	1.81
3	8.4	1.88	1.99	2.33	2.28	1.61
4	19.6	1.91	1.79	1.81	1.90	1.12
6	6.2	1.85	1.97	2.30	2.26	1.48
18	19.4	1.93	1.66	1.61	1.84	1.18
23	5.3	1.77	1.82	2.14	2.12	1.46
29	18.2	1.92	2.02	2.52	2.46	1.58
30	5.3	1.77	1.71	1.96	1.99	1.48

The results are very similar to the results for April 2001, indicating the effectiveness of this approach. The proximity of the flight time allowed us to compare Ne(h)-profiles adapted to the values of

plasma frequencies for both satellites. Examples of such profiles are shown in Fig. 9.

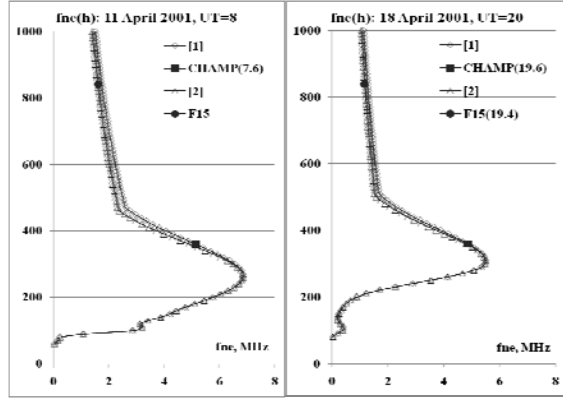


Figure 9: Examples of Ne(h)-profiles adapted to the data of both satellites

An important result is the fact that adaptation to data of various satellites leads to almost the same profile. This suggests that the behavior of the profiles will reflect the real situation. An example of the behavior of profiles during two disturbances in May 2005 is shown in Fig. 10.

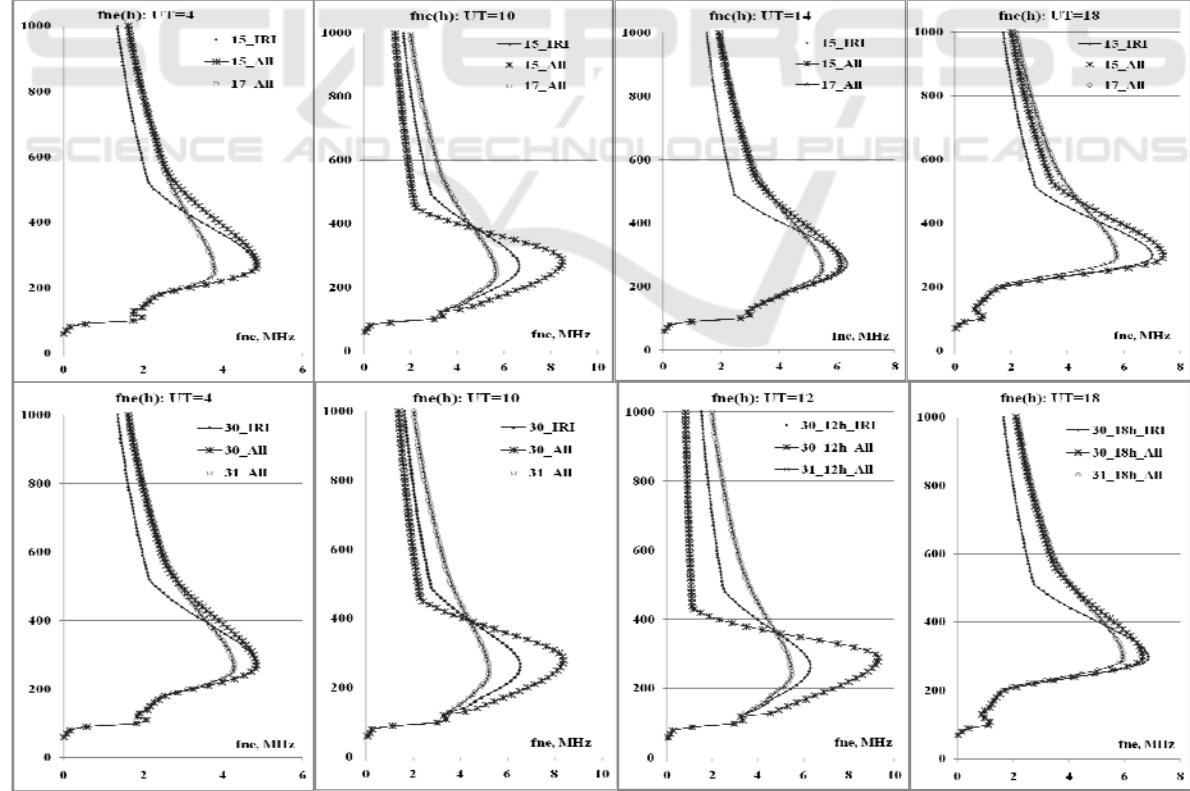


Figure 10: The behavior of the Ne(h)-profiles of the Sofia station during two disturbances in May 2005

Surprising is the identity of changes during these two disturbances, which may indicate some regularities. IRI profiles correspond to quiet conditions. Comparison with these profiles shows that in the early morning hours (UT = 4) on 15 and 30 May at the bottom, the ionosphere is close to the quiet state, and in the topside there is an increase of ionization. On 17 and 31 May, a decrease in the bottom part is observed along with an increase at the topside. This demonstrates the different responses of the upper and lower parts of the ionosphere on the disturbance. In moments of UT = 10 both disturbances are manifested in the form of large increases in the bottom part and the weakening of the ionization at the topside. On May 30 at UT = 12, this process is developing at the time, as on 15 May (chart is not shown), it decays. In UT = 18, both the profiles return back to its original state.

## 7 REFINEMENT OF THE TEC VALUES FROM SATELLITE EXPERIMENTS

Figure 3 shows that there is some variation in correspondence related to the difference in TEC. The difference of the TEC values related to one point and one moment of time is a known fact. The reasons for the differences may be very different. For global maps of JPL (Mannucci et al., 1998), CODE (Schaer et al., 1995), UPC (Hernandez-Pajares et al., 1999), ESA (Sardon et al., 1994; Jakowski et al., 1996), it is the difference in calculation methods. Various receivers may give difference of up to 10 TECU (e.g. Choi et al., 2010). A typical example is Figure 7 of the article (Arikan et al., 2003), which shows the values of TEC, obtained by different methods in the Kiruna station on 25 and 28 April 2001. The values of the global maps for the Sofia station for these two days are shown in Fig. 11.

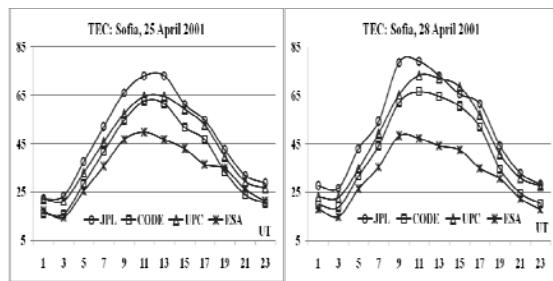


Figure 11: Differences of TEC for the Sofia station calculated from the various global maps

It is seen that the difference in the Sofia station for four maps may lie in the range of 10-30 TECU. In this paper is proposed to specify these values using the plasma frequency on satellites. Fig. 12 shows the values of TEC for four maps and the values obtained by adapting the model to fine on satellites. In the abscissa, day and hour of calculations are indicated.

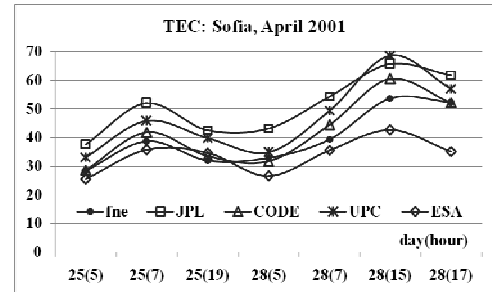


Figure 12: Comparison of TEC calculated from the various global maps with TEC obtained by adaptation to the satellite fine

It is seen that the values of the JPL map are overvalued. It is possible that such adaptation can be used to calibrate the TEC for a given station.

## 8 CONCLUSIONS

The ionosphere is the key factor for the operation of satellite systems. It is one of the largest sources of error in positioning and navigation. The associated error is proportional to the TEC. That is why a lot of attention paid to the development of the ionospheric model. Using the model of Klobuchar (e.g. 1987) allowed to increase the positioning accuracy in 2 times. The next step was done using the IRI model. However, the previous versions of this model also had limitations. This paper highlights the possibilities of a new model (Gulyaeva et al., 2002; Gulyaeva, 2003). They confine to the fact that adaptation of the IRI model to current ionospheric parameters  $foF2$ ,  $hmF2$  and TEC allows us to determine the state of the ionosphere up to altitudes of high-altitude satellites with greater accuracy than ever before. The use of plasma frequency  $fne$ , measured at altitudes of satellites, on the one hand, allows us to validate the model and determine the behavior of the  $Ne(h)$ -profiles, on the other hand, may provide refinement of TEC values which depend on the accuracy of satellite systems from. According to data of the Sofia station, effectiveness of the use of the median equivalent thickness of the

ionosphere  $\tau$  (med) is confirmed not only to fill gaps of foF2 at one station, but also to determine the behavior of foF2 for the other stations in the absence of its experimental data.

## ACKNOWLEDGEMENTS

Authors thank scientists provided data of SPIDR, global maps of TEC, operation and modification of the IRI model, Dr A. Karpachev for CHAMP data.

## REFERENCES

- Araujo-Pradere, E.A., Fuller- Rowell, T.J., Bilitza, D., 2004. Time Empirical Ionospheric Correction Model (STORM) response in IRI2000 and challenges for empirical modeling in the future. *Radio Sci.* 39, RS1S24, doi:10.1029/2002RS002805.
- Arikan, F., Erol, C. B., Arikan, O., 2003. Regularized estimation of vertical total electron content from Global Positioning System data. *J. Geophys. Res.* 108 (A12), 1469, doi:10.1029/2002JA009605.
- Bilitza, D., 2001. International Reference Ionosphere. *Radio Sci.* 36 (2), 261-275.
- Bilitza, D., 2006. The International Reference Ionosphere – Climatological Standard for the Ionosphere. In *Characterising the Ionosphere* (pp. 32-1 – 32-12). *Meeting Proceedings RTO-MP-IST-056, Paper 32. Neuilly-sur-Seine, France: RTO.* Available from: <http://www.rto.nato.int/abstracts.asp>.
- Bilitza, D., 2009. Evaluation of the IRI-2007 Model Options for Topside Electron Density, *Adv. Space Res.*, 44(6), 701–706.
- Bilitza, D., Reinisch, B.W., 2008. International Reference Ionosphere 2007: Improvements and New Parameters. *Adv. Space Res.* 42, 599-609.
- Bilitza, D., Reinisch, B.W., Gulyaeva, T., 2010. ISO technical specification for the ionosphere – IRI recent activities. In *Report presented for COSPAR Scientific Assembly, Bremen, Germany, C01-0004-10.*
- Choi, B.-K., Chung, J.-K., Cho, J.-H., 2010. Receiver DCB estimation and analysis by types of GPS receiver. *J. Astron. Space Sci.*, 27(2), 123-128.
- Gulyaeva, T.L., 2003. International standard model of the Earth's ionosphere and plasmasphere. *Astronomical and Astrophysical Transactions.* 22(4), 639-643.
- Gulyaeva, T.L., Huang, X., Reinisch, B.W., 2002. Ionosphere-plasmasphere software for ISO. *Acta Geod. Geoph. Hung.* 37, 143-152.
- Hernandez-Pajares, M., Juan, J.M., Sanz, J., 1999. New approaches in global ionospheric determination using ground GPS data. *J. Atmos. Sol. Terr. Phys.*, 61, 1237–1247.
- Houminer, Z., Soicher, H., 1996. Improved short –term predictions of foF2 using GPS time delay measurements. *Radio Sci.* 31 (5), 1099-1108.
- Jakowski, N., Sardon, E., Engler, E., Jungstand, A., Klahn, D., 1996. Relationships between GPS-signal propagation errors and EISCAT observations. *Ann. Geophys.*, 14, 1429-1436.
- Klobuchar, J.A., 1987. Ionospheric time-delay algorithm for single-frequency GPS users. *IEEE Transactions on aerospace and electronic systems.* AES-23(3), 325-331.
- Maltseva, O.A., Mozhaeva, N.S., Poltavsky, O.S., Zhabkov, G.A., 2012. Use of TEC global maps and the IRI model to study ionospheric response to geomagnetic disturbances. *Adv. Space Res.* 49, 1076-1087.
- Maltseva, O.A., Zhabkov, G.A., Nikitenko, T.V., 2011. Effectiveness of Using Correcting Multipliers in Calculations of the Total Electron Content according to the IRI2007 Model. *Geomagnetism and Aeronomy*, 51(4), 492–500.
- Mannucci, A. J., Wilson, B. D., Yuan, D. N., Ho, C. H., Lindqwister, U. J., Runge, T. F., 1998. A global mapping technique for GPS-derived ionospheric total electron content measurements. *Radio Science*, 33(3), 565-582.
- McNamara, L.F., 1985. The use of total electron density measurements to validate empirical models of the ionosphere. *Adv. Space Res.* 5(7), 81-90.
- Sardon, E., Rius, A., Zaraoa, N., 1994. Estimation of the receiver differential biases and the ionospheric total electron content from Global Positioning System observations. *Radio Sci.*, 29, 577-586.
- Schaer, S., Beutler, G., Mervart, L., Rothacher, M., Wild, U., 1995. Global and regional ionosphere models using the GPS double difference phase observable. In *IGS Workshop, Potsdam, Germany, May 15-17, 1-16.*
- Stankov, S.M., Jakowski, N., Heise, S., Muhtarov, P., Kutiev, I., Warnant, R., 2003. A New Method for Reconstruction of the Vertical Electron Density Distribution in the Upper Ionosphere and Plasmasphere. *J. Geophys.Res.*, 108, 1164; doi:1029/2002JA009570.
- Uemoto, J., Ono, T., Kumamoto, A., Iizima, M., 2007. Comparison of the IRI 2001 Model with Electron Density Profiles Observed from Topside Sounder On Board the Ohzora (EXOS\_C) and the Akebono (EXOS\_D) Satellites, *Adv. Space Res.*, 39(5), 750–754.
- Zhang, S.-R., Holt, J.M., Bilitza, D., van Eyken, T., McCready, M., Amazory-Mazaudier, C., Fukao, S., Sulzer, M. 2007. Multiple-site comparisons between models of incoherent scatter radar and IRI *Adv. Space Res.* 39, 910-917.